

Supplemental Materials

Neural responses to exclusion predict susceptibility to social influence

Emily B. Falk, Christopher N. Cascio, Matthew Brook O'Donnell, Joshua Carp, Francis J. Tinney, Jr., C. Raymond Bingham, Jean T. Shope, Marie Claude Ouimet, Anuj K. Pradhan, Bruce G. Simons-Morton

SUPPLEMENTAL METHODS

Participants. Sixty-six adolescent males (highest risk group for crash) were recruited for a larger study on the effects of peer influence on recently-licensed male teen drivers (Simons-Morton et al., in press). A subset of 43 participants was invited to participate in the fMRI portion of the study. Seven participants were excluded from the analyses. One participant began the fMRI study, but was excluded based on parent report of non-neurotypicality (Autism spectrum diagnosis) at the start of the session. Five additional participants underwent fMRI but did not complete the driving simulator portion of the study due to either simulator sickness (similar to motion sickness, but in the simulator) or technical problems recording driving data, and one participant was excluded due to issues with fMRI data pre-processing (more specifically, this participant's data were unable to be processed using the robust weighted least squares toolbox, such that the algorithm crashed each time it reached this participant's data). The remaining thirty-six neurotypical adolescent males aged 16-17 years ($M = 16.8$, $SD = .47$) successfully completed both an fMRI session at the University of Michigan fMRI Center as well as a separate driving simulator appointment at the University of Michigan Transportation Research Institute (UMTRI). Within the 4-9 months prior to the scan, all participants had obtained a Level 2 (intermediate) Michigan driver license allowing them to drive independently, but with passenger and night driving restrictions. Participants were eligible if they were right handed, did not suffer from claustrophobia, were not currently taking any psychoactive medications, had normal (or

corrected to normal) vision, did not have metal in their body that was contraindicated for fMRI, and did not typically experience motion sickness. Legal guardians provided written informed consent following telephone discussion with a trained research assistant, and teens provided written assent. Both parents and teens were given an opportunity to ask questions about the study prior to the first appointment.

Cyberball. Cyberball is a game that allows simulation of both inclusion and exclusion in an fMRI environment (Eisenberger, Lieberman, & Williams, 2003; Williams, Cheung, & Choi, 2000). In this task, participants believe they are engaging in a virtual ball-tossing game with the two “participant” confederates introduced at the start of the session. In reality, a pre-set computer program controls the other two virtual players. During the first part of the game, both other players throw to one another and to the participant equally. After several rounds, however, the other players stop throwing the ball to the participant and only throw to one another.

Participants and confederates were introduced to Cyberball as a “virtual ball tossing game” during the initial introduction before the scan. The controls for Cyberball (i.e., which buttons control throwing to each other player) were also explained during this initial group instruction period. During the fMRI scan, participants were reminded of these instructions, and completed two rounds of the game (inclusion and exclusion). The two rounds of Cyberball each lasted 178 seconds. A fair game was always played first, in which all participants received the ball equally often. This was followed by an unfair game, in which all participants start out receiving the ball equally often, but where the participant is left out after a few throws. Order of the rounds was held constant to preserve the psychological experience across participants. These rounds were preceded by a period in which participants visually tracked a star as it moved on the

screen (105 seconds). Each of these periods was separated by a 16 second dot-fixation rest period.

At the end of the fMRI session, participants were probed for suspicion and told that there had been a computer glitch that prevented other participants from throwing the ball to them. This was done to relieve distress of exclusion. A full debrief did not take place immediately to preserve integrity of the remainder of the study, but instead was conducted at the end of the study via regular mail or email.

Self-report measures. The susceptibility to peer pressure (SPP) scale includes 11 questions in which participants indicate how willing they would be to engage in a range of behaviors if each were suggested by a friend. Example questions include: i) *If a friend offered you a drink at a party, would you "want" to take it? ; ii) If your best friend is skipping school, would you? ; iii) If you got in a car driven by a friend who is not wearing a safety belt, would you buckle your safety belt?* Participants' response options included: no, probably not, probably, yes (scored 1-4). Higher scores on this measure indicate increased susceptibility to peer pressure. For the resistance to peer influence (RPI) scale participants were instructed to choose between two statements. Example comparisons include: i) *Some people go along with their friends just to keep their friends happy. Other people refuse to go along with what their friends want to do, even though they know it will make their friends unhappy;* ii) *Some people hide their true opinion from their friends if they think their friends will make fun of them because of it. Other people will say their true opinion in front of their friends, even if they know their friends will make fun of them because of it.* After selecting which statement best represented them, participants were asked whether the chosen statement was "sort of true" or "really true" of them (scored 1-4). Higher scores on this measure indicate greater ability to resist peer influence. For the distress

during exclusion (need/threat) scale (NTS) participants are instructed to rate their level of agreement with the statements on a seven-point scale ranging from “strongly disagree” to “strongly agree”. Example statements include: i) *I had the feeling that I failed during the game;* ii) *I believed that my contribution to the game did not matter; and iii) During the game it felt as if my presence was not meaningful* (note: participants completed the full scale as administered by van Beest and Williams (2006)). Lower scores indicate greater feelings of threat or distress and higher scores indicate greater need satisfaction.

fMRI Scanning Parameters. Functional images were recorded using a reverse spiral sequence (TR = 2000 ms, TE = 30 ms, flip angle = 90°, 43 axial slices, FOV = 220 mm, 3 mm thick; voxel size = 3.44 x 3.44 x 3.0 mm). We also acquired in-plane T1-weighted images (43 slices; slice thickness = 3 mm; voxel size = .86 x .86 x 3.0mm) and high-resolution T1-weighted images (SPGR; 124 slices; slice thickness = 1.02 x 1.02 x 1.2 mm) for use in coregistration and normalization.

fMRI Preprocessing. To allow for the stabilization of the BOLD signal, the first four volumes (eight seconds) of each run were discarded prior to analysis. Functional images were despiked using the 3dDespike program as implemented in the AFNI toolbox. Next, data were corrected for differences in the time of slice acquisition using sinc interpolation; the first slice served as the reference slice. Data were then spatially realigned to the first functional image. We then coregistered the functional and structural images using a two-stage procedure. First, in-plane T1 images were registered to the mean functional image. Next, high-resolution T1 images were registered to the in-plane image. After coregistration, high-resolution structural images were skull-stripped using the VBM8 toolbox for SPM (<http://dbm.neuro.uni-jena.de/vbm>), and then

normalized to the skull-stripped MNI template provided by FSL (“MNI152_T1_1mm_brain.nii”). Finally, functional images were smoothed using a Gaussian kernel (8 mm FWHM).

fMRI First Level Modeling. Three phases of cyberball (inclusion, exclusion, visual tracking) were modeled as blocks and convolved with the synthetic hemodynamic response as provided by SPM. The six rigid-body translation and rotation parameters derived from spatial realignment were also included as nuisance regressors. Data were high-pass filtered with a cutoff of 128 s. Volumes were weighted according to the inverse of their noise variance using the robust weighted least squares toolbox (Diedrichsen & Shadmehr, 2005). This procedure reduces the effects of head motion and other sources of noise on estimates of brain activation (<http://www.icn.ucl.ac.uk/motorcontrol/imaging/robustWLS.html>).

fMRI Regions of Interest. Anatomical regions of interest (ROIs) were constructed in Wake Forest University Pickatlas toolbox within SPM (Maldjian, Laurienti, Kraft, & Burdette, 2003), combining gross definitions from the Automated Anatomical Labeling Atlas (AAL; (Tzourio-Mazoyer et al., 2002), Brodmann areas, and manual tracing, intersected with x,y,z bounds as noted below to restrict sub-regions. MarsBar (Brett, Anton, Valabregue, & Poline, 2002) was used to convert these anatomical images to ROIs.

Social pain network: The hypothesized social pain network was constructed to include bilateral anterior insula, the subgenual cingulate cortex, and the dorsal anterior cingulate cortex.

Anterior insula: The anterior insula ROI was defined as all voxels within the left and right insula masks provided by PickAtlas that were anterior to the $y=0$ plane.

Dorsal ACC: The dACC ROI was defined as the union of Brodmann areas 24 and 32 (dilated to 2mm), as well as the anterior, middle, and posterior cingulate masks from the AAL atlas. We then subtracted Brodmann areas 8 and 9 from this mask. Finally, we restricted this ROI to the voxels bounded by ($x=-16$ to 16, $y=0$ to 33, and $z=6$ to 52).

Subgenual ACC: The subgenual ACC ROI was manually traced to include regions of the cingulate and paracingulate cortices ventral to the body of the corpus callosum and posterior to the genu.

Mentalizing network: The mentalizing network was constructed to include the union of rTPJ, DMPFC, and PC

Right TPJ: The right TPJ ROI was defined as all voxels within Brodmann areas 22, 39, and 40 intersected with a box-shaped mask centered at ($x = 60$, $y = -52$, $z = 30$) and extending 40, 16, and 24 mm along the x, y, and z axes, respectively.

DMPFC: The DMPFC ROI was defined as all voxels within Brodmann areas 8 and 9 intersected with a box-shaped mask centered at ($x = 0$, $y = 52$, $z = 50$) and extending 40, 44, and 48 mm along the x, y, and z axes, respectively.

PCC: The PCC ROI was defined as the union of the left and right posterior cingulate, as defined by the AAL atlas.

Driving Simulator. The UMTRI facilities include a high fidelity, fixed-base driving simulator (Figure 2) manufactured by DriveSafety, with a cab consisting of the front three-quarters of the body and front interior of a sedan. The simulator is situated in a dedicated lab space with a computer-controlled, projected LCD instrument cluster, operating foot controls, and a torque motor providing realistic steering force feedback. Road scenes were projected at a resolution of 1024 X 768 pixels on each of three forward screens located 4.9 meters from the driver and a rear screen located 3.7 meters behind, providing 120 degrees of wrap-around forward view, and a road scene visible through the side and rearview mirrors for an additional 40 degrees of rear field view. The car was also equipped with a sound system that produced both exterior and interior sounds, as well as road vibration through the floorboard.

Virtual Driving Environment. The simulated drives were created to reflect a high degree of ecological validity with the real driving environment. Simulated worlds thus contained standard roadways, intersections, traffic control devices, other visual elements (e.g., vegetation, buildings, sky), and other road users including vehicles and pedestrians. These worlds were custom created from a library of environments and can include various scenes (rural, urban, suburban etc), as well as programmable traffic flow, individual road users, and other elements such as signal phase.

Driving worlds and scenarios. The three simulated worlds for this study and the scenarios they contained were programmed using Drive Safety software. The first world was a 5-10 minute practice/coaching drive that allowed the participant to acclimatize to the simulator. The other two worlds were the experimental worlds (World A & World B), each taking about

15-20 minutes to drive and containing an urban setting with a series of signalized intersections, ambient traffic and relevant environmental elements (e.g., buildings, trees, signs, pedestrians).

Various *scenarios*, which are dynamic features within the simulated world that respond to driver behavior in a specific manner each time they are encountered and elicit specific driver responses, were programmed into each world. Scenarios in this study were traffic light phase changes programmed to begin when the simulated vehicle was within a certain temporal distance of an intersection. The scenarios in this study caused the participant to decide whether to stop at an amber light or continue and risk remaining in the intersection when the light turned red.

The two simulated worlds contained 42 identical four-way signalized intersections spaced 200 meters apart, but presented in reverse orders and orientations to provide the same experience without being identical in the two drives. In both worlds a lead vehicle was present to limit speed and provide direction, and participants were instructed to follow the lead vehicle. Traffic lights at the intersections were pseudo-randomly assigned to be green, yellow or red as the driver approached them. Some of the traffic lights remained green while others changed to yellow and then red. The distance at which the driver triggered the phase change from green to yellow and the length of the yellow phase were programmed to vary across intersections so that sometimes the driver had ample time to stop, while at other times had to decide quickly whether to stop or continue. Dilemmas posed by a phase change to yellow are common experiences of everyday driving and relevant to safety (Gazis, Herman, & Maradudin, 1960). The scenarios were designed to cause changes in driver responses by varying the length of the yellow and red light phases, such that lights turned yellow at 6.0, 3.4, 3.0, or 2.4 seconds before the vehicle entered the intersection. There were 23 intersections with the four light phase timings 5 intersections with the 6.0-second timings, and 6 intersections each with the 3.4-, 3.0-, and 2.6-second timings. The remaining intersections were in a 'green wave' and without the lead vehicle to allow

variation in speed. The dependent variables were calculated using the data from the 18 intersections with the 3.4-, 3.0-, and 2.6-second timings, as there was no variability in the 6.0 second timed lights.

The simulated worlds were programmed with clear daylight conditions and dry roads. All the elements in the worlds, such as moving traffic and pedestrians, were programmed to minimize the chance of crashes, loss of control, or other events that would interrupt the drive.

Driving simulator data collection and extraction. The driving simulator recorded vehicle performance data at 60 Hz. The dependent variables were calculated using the data from the programmed intersections within each drive. A trained simulator data coder calculated the combined time spent in all 18 intersections while the light was red, the percentage of the 18 intersections at which the participant failed to stop when the light was yellow (failed to stop), and the percentage of time spent in the intersection during the red light phase calculated by dividing the time spent in the intersection during the red light phase by the total time in intersection and averaging across all 18 intersections (percent red). The current manuscript focuses on the “percent red” metric. However, all results reported are qualitatively unchanged when calculated using the “failed to stop” metric (see table S3). Using raw total time, effect sizes are attenuated, but in the same direction as reported results (see table S4). This attenuation is likely due to the fact that raw time in intersection is a function of two competing factors: running red/yellow lights and driving speed (which is accounted for in the percent measures).

Supplementary Results

Sub-region analyses

Table S1 (Sub-regions analysis): Relationship between neural activity in the sub-regions of the social pain network (subACC, AI, and dACC) during Cyberball and risk-taking (percent red) in the presence of peers in the driving simulator session, controlling for passenger type, drive order, and solo risk-taking behavior (as measured by performance in the solo drive at the simulator).

Table S1a. Effect of anatomical neural activity in the subgenual cingulate (subACC).

| Variable | Unstandardized Coefficients | | Standardized Coefficients | | |
|----------------|-----------------------------|------------|---------------------------|------------------------------|--------|
| | B | Std. Error | Beta | t | Sig. |
| Drive Order | 0.042 | 0.036 | 0.128 | 1.184 | 0.245 |
| Passenger Type | 0.088 | 0.035 | 0.269 | 2.506 | 0.018 |
| Solo Drive | 0.73 | 0.131 | 0.63 | 5.589 | < .001 |
| Cyber (subACC) | 0.069 | 0.022 | 0.316 | 3.123 | 0.004 |
| | | | <i>N</i> = 36 | <i>Model R Square</i> = .719 | |

Table S1b. Effect of anatomical neural activity in the anterior insula (AI).

| Variable | Unstandardized Coefficients | | Standardized Coefficients | | |
|----------------|-----------------------------|------------|---------------------------|------------------------------|--------|
| | B | Std. Error | Beta | t | Sig. |
| Drive Order | 0.02 | 0.036 | 0.062 | 0.558 | 0.581 |
| Passenger Type | 0.081 | 0.037 | 0.248 | 2.229 | 0.033 |
| Solo Drive | 0.81 | 0.133 | 0.698 | 6.103 | < .001 |
| Cyber (AI) | 0.107 | 0.042 | 0.267 | 2.552 | 0.016 |
| | | | <i>N</i> = 36 | <i>Model R Square</i> = .695 | |

Table S1c. Effect of anatomical neural activity in the dorsal anterior cingulate cortex (dACC).

| Variable | Unstandardized Coefficients | | Standardized Coefficients | | |
|----------------|-----------------------------|------------|---------------------------|------------------------------|--------|
| | B | Std. Error | Beta | t | Sig. |
| Drive Order | 0.015 | 0.039 | 0.045 | 0.386 | 0.702 |
| Passenger Type | 0.071 | 0.038 | 0.216 | 1.861 | 0.072 |
| Solo Drive | 0.835 | 0.14 | 0.72 | 5.976 | < .001 |
| Cyber (dACC) | 0.059 | 0.035 | 0.187 | 1.698 | 0.1 |
| | | | <i>N</i> = 36 | <i>Model R Square</i> = .662 | |

Table S1d. Effect of functional neural activity in the subgenual cingulate (subACC).

| Variable | Unstandardized Coefficients | | Standardized Coefficients | | |
|---------------------|-----------------------------|------------|---------------------------|------------------------------|--------|
| | B | Std. Error | Beta | t | Sig. |
| Drive Order | 0.045 | 0.034 | 0.138 | 1.314 | 0.198 |
| Passenger Type | 0.082 | 0.033 | 0.251 | 2.465 | 0.019 |
| Solo Drive | 0.72 | 0.127 | 0.621 | 5.692 | < .001 |
| Cyber fROI (subACC) | 0.084 | 0.024 | 0.341 | 3.54 | 0.001 |
| | | | <i>N</i> = 36 | <i>Model R Square</i> = .737 | |

Table S1e. Effect of functional neural activity in the anterior insula (AI).

| Variable | Unstandardized Coefficients | | Standardized Coefficients | | |
|-----------------|-----------------------------|------------|---------------------------|------------------------------|--------|
| | B | Std. Error | Beta | t | Sig. |
| Drive Order | 0.01 | 0.034 | 0.031 | 0.296 | 0.769 |
| Passenger Type | 0.075 | 0.033 | 0.227 | 2.241 | 0.032 |
| Solo Drive | 0.803 | 0.125 | 0.692 | 6.442 | < .001 |
| Cyber fROI (AI) | 0.089 | 0.026 | 0.326 | 3.402 | 0.002 |
| | | | <i>N</i> = 36 | <i>Model R Square</i> = .731 | |

Table S2 (sub-region analysis): Relationship between neural activity in the sub-regions of the mentalizing network (DMPFC, rTPJ, and PCC) during Cyberball and risk-taking (percent red) in the presence of peers in the driving simulator session, controlling for passenger type, drive order, and solo risk-taking behavior (as measured by performance in the solo drive at the simulator).

Table S2a. Effect of anatomical neural activity in the dorsal medial prefrontal cortex (DMPFC).

| Variable | Unstandardized Coefficients | | Standardized Coefficients | | |
|----------------|-----------------------------|------------|---------------------------|------------------------------|--------|
| | B | Std. Error | Beta | t | Sig. |
| Drive Order | 0.005 | 0.038 | 0.014 | 0.126 | 0.9 |
| Passenger Type | 0.072 | 0.036 | 0.221 | 1.994 | 0.055 |
| Solo Drive | 0.832 | 0.135 | 0.718 | 6.177 | < .001 |
| Cyber (DMPFC) | 0.053 | 0.023 | 0.247 | 2.315 | 0.027 |
| | | | <i>N</i> = 36 | <i>Model R Square</i> = .685 | |

Table S2b. Effect of anatomical neural activity in the right temporal parietal junction (rTPJ).

| Variable | Unstandardized Coefficients | | Standardized Coefficients | | |
|----------------|-----------------------------|------------|---------------------------|------------------------------|--------|
| | B | Std. Error | Beta | t | Sig. |
| Drive Order | 0.017 | 0.036 | 0.052 | 0.474 | 0.639 |
| Passenger Type | 0.073 | 0.035 | 0.221 | 2.065 | 0.047 |
| Solo Drive | 0.815 | 0.131 | 0.703 | 6.226 | < .001 |
| Cyber (rTPJ) | 0.101 | 0.037 | 0.275 | 2.743 | 0.01 |
| | | | <i>N</i> = 36 | <i>Model R Square</i> = .703 | |

Table S2c. Effect of anatomical neural activity in the posterior cingulate cortex (PCC).

| Variable | Unstandardized Coefficients | | Standardized Coefficients | | |
|----------------|-----------------------------|------------|---------------------------|------------------------------|--------|
| | B | Std. Error | Beta | t | Sig. |
| Drive Order | 0.02 | 0.037 | 0.062 | 0.556 | 0.582 |
| Passenger Type | 0.067 | 0.036 | 0.204 | 1.883 | 0.069 |
| Solo Drive | 0.765 | 0.136 | 0.66 | 5.639 | < .001 |
| Cyber (PCC) | 0.073 | 0.03 | 0.251 | 2.445 | 0.02 |
| | | | <i>N</i> = 36 | <i>Model R Square</i> = .690 | |

Table S2d. Effect of functional neural activity in the dorsal medial prefrontal cortex (DMPFC).

| Variable | Unstandardized Coefficients | | Standardized Coefficients | | |
|--------------------|------------------------------------|-------------------|----------------------------------|------------------------------|-------------|
| | B | Std. Error | Beta | t | Sig. |
| Drive Order | -0.01 | 0.037 | -0.03 | -0.264 | 0.793 |
| Passenger Type | 0.069 | 0.034 | 0.21 | 2.022 | 0.052 |
| Solo Drive | 0.839 | 0.128 | 0.723 | 6.543 | < .001 |
| Cyber fROI (DMPFC) | 0.066 | 0.022 | 0.311 | 3.036 | 0.005 |
| | | | <i>N = 36</i> | <i>Model R Square = .715</i> | |

Table S2e. Effect of functional neural activity in the right temporal parietal junction (rTPJ).

| Variable | Unstandardized Coefficients | | Standardized Coefficients | | |
|-------------------|------------------------------------|-------------------|----------------------------------|------------------------------|-------------|
| | B | Std. Error | Beta | t | Sig. |
| Drive Order | 0.026 | 0.038 | 0.08 | 0.699 | 0.49 |
| Passenger Type | 0.057 | 0.036 | 0.172 | 1.566 | 0.128 |
| Solo Drive | 0.778 | 0.139 | 0.671 | 5.59 | < .001 |
| Cyber fROI (rTPJ) | 0.055 | 0.028 | 0.208 | 1.994 | 0.055 |
| | | | <i>N = 36</i> | <i>Model R Square = .673</i> | |

Additional DVs

Two additional dependent measures of risk were collected during the simulator session: the proportion of time participants did not stop at an intersection with a yellow light (failed to stop), and the total time that participants were in the intersection during a red light (total red). Results from primary analyses reported in the main body of the manuscript are consistent directionally with all results computed (increased activity in social pain and mentalizing networks was positively related to risk taking in the presence of peers, controlling for solo risk taking and other relevant metrics). Although results from the “total time” measures are in the same direction as other relevant driving measures, they are not significant in these models. Inconsistencies between our total time measure and the proportion based measures likely have to do with the fact that our total time measure is confounded by driving speed (as faster moving vehicles may show less time in an intersection than a slower moving vehicle, thus appearing to behave in a safer manner, and making results more difficult to interpret). Results are reported here for comprehensiveness/ transparency.

Table S3 (Additional DVs): Relationship between neural activity in the social pain network during Cyberball and risk-taking in the presence of peers in the driving simulator session, controlling for passenger type, drive order, and solo risk-taking behavior (as measured by performance in the solo drive at the simulator).

Table S3a. Effect of neural activity in the social pain network (anterior insula (AI) and subgenual cingulate (subACC)).

| Variable | Unstandardized Coefficients | | Standardized Coefficients | | |
|---------------------|-----------------------------|------------|---------------------------|------------------------------|--------|
| | B | Std. Error | Beta | t | Sig. |
| Drive Order | -0.025 | 0.047 | -0.055 | -0.527 | 0.602 |
| Passenger Type | -0.14 | 0.048 | -0.311 | -2.946 | 0.006 |
| Solo Drive | 0.749 | 0.12 | 0.671 | 6.248 | < .001 |
| Cyber (AI & subACC) | -0.162 | 0.052 | -0.311 | -3.138 | 0.004 |
| | | | <i>N</i> = 36 | <i>Model R Square</i> = .733 | |

Table S3b. Effect of neural activity in the social pain network (anterior insula (AI) and subgenual cingulate (subACC)).

| Variable | Unstandardized Coefficients | | Standardized Coefficients | | |
|---------------------|-----------------------------|------------|---------------------------|------------------------------|-------|
| | B | Std. Error | Beta | t | Sig. |
| Drive Order | 4.148 | 2.913 | 0.228 | 1.424 | 0.164 |
| Passenger Type | 4.271 | 2.936 | 0.235 | 1.455 | 0.156 |
| Solo Drive | 0.513 | 0.213 | 0.398 | 2.41 | 0.022 |
| Cyber (AI & subACC) | 2.303 | 3.169 | 0.11 | 0.727 | 0.473 |
| | | | <i>N</i> = 36 | <i>Model R Square</i> = .368 | |

Table S4 (Additional DVs): Relationship between neural activity in the mentalizing network during Cyberball and risk-taking in the presence of peers in the driving simulator session.

Table S4a. Effect of neural activity in the mentalizing network (dorsal medial prefrontal cortex (DMPFC), right temporal parietal junction (rTPJ), and posterior cingulate (PCC)).

| Variable | Unstandardized Coefficients | | Standardized Coefficients | | Sig. |
|----------------------------|-----------------------------|------------|---------------------------|------------------------------|--------|
| | B | Std. Error | Beta | t | |
| Drive Order | 0.007 | 0.049 | 0.014 | 0.134 | 0.894 |
| Passenger Type | -0.12 | 0.047 | -0.266 | -2.532 | 0.017 |
| Solo Drive | 0.792 | 0.122 | 0.709 | 6.476 | < .001 |
| Cyber (DMPFC, rTPJ, & PCC) | -0.11 | 0.04 | -0.277 | -2.741 | 0.01 |
| | | | <i>N</i> = 36 | <i>Model R Square</i> = .717 | |

Table S4b. Effect of neural activity in the mentalizing network (dorsal medial prefrontal cortex (DMPFC), right temporal parietal junction (rTPJ), and posterior cingulate (PCC)).

| Variable | Unstandardized Coefficients | | Standardized Coefficients | | Sig. |
|----------------------------|-----------------------------|------------|---------------------------|------------------------------|-------|
| | B | Std. Error | Beta | t | |
| Drive Order | 3.488 | 2.923 | 0.192 | 1.193 | 0.242 |
| Passenger Type | 4.277 | 2.818 | 0.235 | 1.518 | 0.139 |
| Solo Drive | 0.529 | 0.21 | 0.41 | 2.522 | 0.017 |
| Cyber (DMPFC, rTPJ, & PCC) | 2.636 | 2.388 | 0.164 | 1.104 | 0.278 |
| | | | <i>N</i> = 36 | <i>Model R Square</i> = .382 | |

Main effects of Cyberball (Exclusion > Inclusion)

Table S5 (Activation in Cyberball): Regions associated with the main effect of exclusion > inclusion during Cyberball.

Table S5a. Results from a whole brain search for activation associated with exclusion > inclusion (thresholded at $p < .005$, $K = 36$, corresponding to corrected $p < .05$)

| Region | Local Max (x y z) | Cluster size | t-stat |
|-------------------------|-------------------|--------------|--------|
| Anterior Insula (Right) | 25 19 -11 | 971 | 4.92 |
| Anterior Insula (Left) | -23 19 -11 | - | 4.89 |
| SubACC | 1 26 -2 | - | 4.79 |
| DMPFC | -2 67 28 | - | 4.07 |
| Cuneus (Right) | 15 -98 25 | 48 | 3.92 |
| MTG (Left) | -57 -30 -8 | 342 | 5.2 |

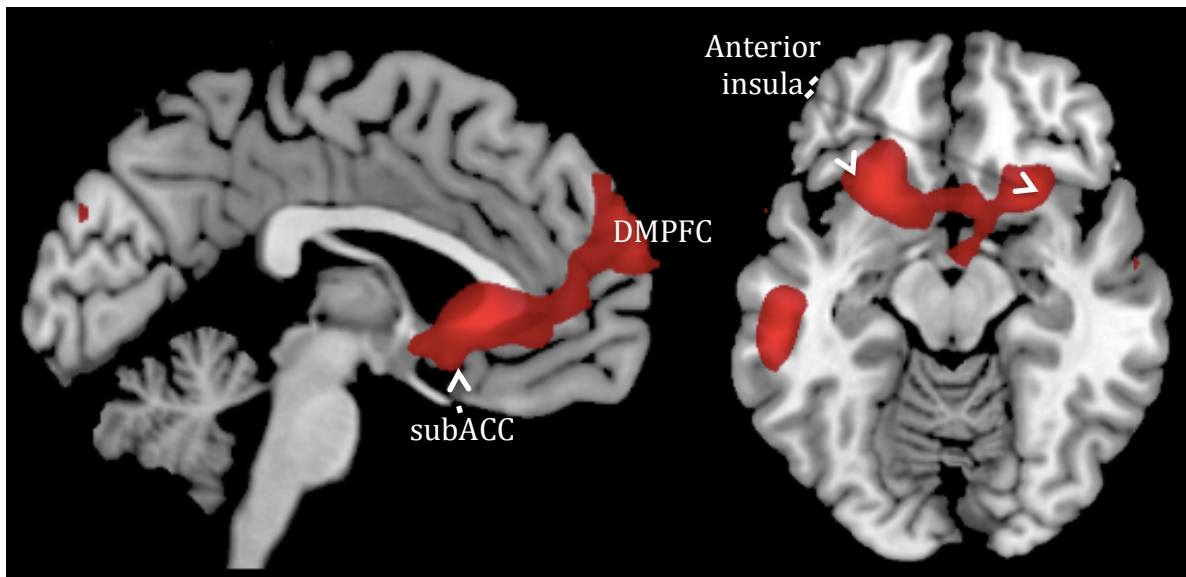


Table S5b. Clusters constrained by anatomical mask of the hypothesized social pain network (thresholded at $p < .005$, $K = 10$; Figure 4a)

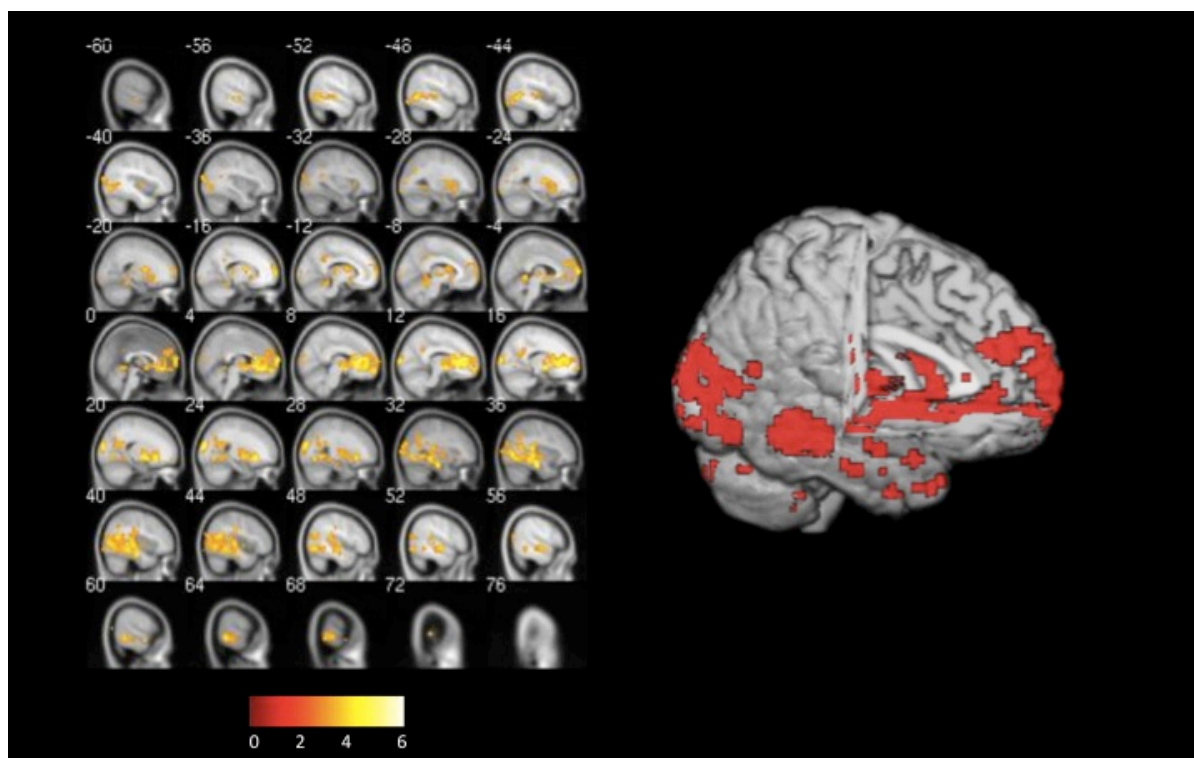
| Region | Local Max (x y z) | Cluster size | t-stat |
|--------------------------|-------------------|--------------|--------|
| Subgenual ACC | 1 22 -2 | 88 | 4.62 |
| Anterior Insular (Left) | -26 22 -11 | 27 | 4.57 |
| Anterior Insular (Right) | 25 19 -11 | 21 | 4.52 |

Table S5c. Clusters constrained by anatomical mask of the hypothesized mentalizing network (thresholded at $p < .005$, $K = 10$; Figure 6a)

| Region | Local Max (x y z) | Cluster size | t-stat |
|-------------|-------------------|--------------|--------|
| DMPFC | -2 67 28 | 57 | 4.07 |
| TPJ (Right) | 60 -60 37 | 11 | 3.57 |

Table S6. Correlation between neural activity during exclusion > inclusion during cyberball and increased risk taking during passenger > solo drives in the driving simulator (thresholded at $p < .005$, $k=36$).

| Region | Local Max | Cluster size | t-stat |
|-----------------------------------|------------|--------------|--------|
| DMPFC | -2 56 28 | 4019 | 3.25 |
| pSTS/ TPJ | 49 -32 13 | - | 3.41 |
| SubACC | 4 28 -5 | - | 4.84 |
| Anterior insula | -29 18 4 | - | 3.17 |
| Anterior insula | 32 22 -2 | - | 3.20 |
| dACC | 1 18 22 | - | 2.79 |
| Parahippocampal gyrus | 35 -19 -20 | - | 5.55 |
| Ventral striatum | 15 -2 -2 | - | 6 |
| MPFC | 4 70 7 | - | 4.86 |
| Parahippocampal gyrus | 35 -19 -20 | - | 5.55 |
| Cuneus | 25 -88 19 | - | 5.21 |
| Inferior temporal gyrus | -47 -64 -5 | 378 | 4.32 |
| Middle temporal gyrus | -57 -19 -5 | - | 4 |
| Posterior superior temporal gyrus | -43 -26 4 | - | 2.73 |
| Precuneus | -26 -67 31 | 43 | 3.3 |
| Medial temporal lobe | -33 -54 19 | - | 3.27 |
| Inferior occipital cortex | -9 -98 7 | 40 | 3.23 |



Slice view and rendered view of results described in Table S6 ($p < .005$, $k=36$, colorbar represents t-vals)

References

- Brett, M, Anton, J, Valabregue, R, & Poline, J (2002). *Region of interest analysis using an SPM toolbox*. Paper presented at the The 8th International Conference on Functional Mapping of the Human Brain, Sendai, Japan.
- Diedrichsen, Jörn, & Shadmehr, Reza. (2005). Detecting and adjusting for artifacts in fMRI time series data. *NeuroImage*, 27(3), 624-634. doi: 10.1016/j.neuroimage.2005.04.039
- Eisenberger, N. I., Lieberman, M. D., & Williams, K. D. (2003). Does rejection hurt? An FMRI study of social exclusion. *Science*, 302(5643), 290-292. doi10.1126/science.1089134
- Gazis, D., Herman, R., & Maradudin, A. (1960). The problem with the amber signal light in traffic flow. *Operations Research*, 8(1), 112-132.
- Maldjian, J. A., Laurienti, P. J., Kraft, R. A., & Burdette, J. H. (2003). An automated method for neuroanatomic and cytoarchitectonic atlas-based interrogation of fMRI data sets. *Neuroimage*, 19(3), 1233-1239. doi: S1053811903001691 [pii]
- Simons-Morton, B., Bingham, R., Falk, E. B., Ouimet, M. C., Pradhan, A., Shope, J., . . . Green, P. (in press). The effect of teenage passengers on simulated driving among teenagers: Social normative influences. *Health Psychology*.
- Tzourio-Mazoyer, N., Landeau, B., Papathanassiou, D., Crivello, F., Etard, O., Delcroix, N., . . . Joliot, M. (2002). Automated anatomical labeling of activations in SPM using a macroscopic anatomical parcellation of the MNI MRI single-subject brain. *Neuroimage*, 15(1), 273-289. doi: S1053811901909784 [pii]
- Williams, K. D., Cheung, C. K., & Choi, W. (2000). Cyberostracism: effects of being ignored over the Internet. *J Pers Soc Psychol*, 79(5), 748-762.